Urban Tree Canopy Change Assessment: City of Asheville, NC (2022–2025)

Report Date: May 14, 2026

Prepared for:

The City of Asheville

Prepared by:

Skytec LLC
1100 Market St. Suite 200
Chattanooga, Tennessee 37402
(423) 521-2683





Contents

1 Introduction 1
2 Data and Methods 1
2.1 Study Area 1
2.2 Imagery Sources 1
2.2.1 2022 NAIP Baseline Imagery 1
2.2.2 2025 High-Resolution Orthomosaic Imagery 2
2.3 Study Area Maps 2
Figure 1. Study Area Map: 2022 NAIP Imagery 3
Figure 2. Study Area Map: 2025 High-Resolution Orthomosaic 4
2.4 Data Preparation and Harmonization 5
2.5 Image Classification 5
2.6 Manual Tree Canopy Clean Up 6
2.7 Data Considerations and Limitations 6
2.8 Role of the Data in This Assessment 7
3 Urban Tree Canopy Assessment 8
3.1 Urban Tree Canopy Extent 8
Figure 3. Urban tree canopy coverage, Asheville, NC (2022–2025) 8
3.2 Canopy Change Analysis 9
Figure 4. Classified Tree Canopy: 2022 NAIP Imagery 10
Figure 5. Classified Tree Canopy: 2025 High-Resolution Imagery 11
3.3 Spatial Patterns 12
Figure 6. Canopy Change Map: 2022 to 2025 13
Figure 7a. Canopy Change Inset A: Commercial and Residential Land Clearing 14
Figure 7b. Canopy Change Inset B: Residential Neighborhood Loss 14
Figure 7c. Canopy Change Inset C: Riparian Corridor and Recreation Area 15
Figure 7d. Canopy Change Inset D: Airport Perimeter Area 16
4 Discussion 17
5 Appendix 19
Table A1. Esri High Resolution Land Cover Classification Model Validation Metrics 19
Table A2. Imagery Source Spectral Band Configurations 19
References 20

1 Introduction

Urban forests are a foundational component of resilient, livable cities. The distribution and density of tree canopy directly influence environmental performance, public health outcomes, and long-term sustainability. Urban tree canopy (UTC), the layer of leaves, branches, and stems that covers the ground when viewed from above, is an important measure of ecological health in urban areas.

Trees provide measurable ecosystem services including reduction of urban heat island effects, stormwater interception, air pollutant removal, carbon sequestration, energy savings, and improved quality of life.

Extreme weather events can significantly disrupt these benefits. Hurricane Helene presents a case study in how severe disturbances impact urban canopy systems and necessitate rapid, data-driven assessment.

This project delivers a post-event urban canopy assessment for the City of Asheville, North Carolina, leveraging high-resolution satellite imagery. The analysis compares baseline (2022) and post-event (2025) conditions.

The objectives of this study are to:

- Quantify urban tree canopy extent before and after Hurricane Helene
- Identify spatial patterns of canopy loss and gain
- Support municipal planning and recovery strategies

2 Data and Methods

2.1 Study Area

The study area for this assessment is the full administrative extent of the City of Asheville, North Carolina, covering approximately 29,279.41 acres (about 118.5 km^2). The project area includes a diverse mix of land cover types, including dense urban development, residential neighborhoods, transportation corridors, riparian systems, maintained open spaces, and forested terrain. This landscape variability makes Asheville well suited for high-resolution urban canopy analysis and requires a classification workflow capable of distinguishing fine-scale differences in vegetation and developed land cover.

This analysis was conducted at the request of the city of Asheville to evaluate citywide urban tree canopy conditions following Hurricane Helene and to establish a consistent basis for comparing pre- and post-event imagery. All imagery and derivative products used in this study were clipped to the official City of Asheville boundary to maintain spatial consistency throughout the analysis.

2.2 Imagery Sources

Two primary imagery datasets were used in this assessment: a 2022 baseline dataset derived from the National Agriculture Imagery Program (NAIP), and a 2025 post-event high-resolution orthomosaic assembled from commercial satellite and orthorectified imagery sources.

2.2.1 2022 NAIP Baseline Imagery

The baseline imagery used for pre-event comparison consists of 2022 NAIP imagery [USDA Farm Service Agency, 2022] with an original spatial resolution of approximately 60 centimeters. NAIP imagery is collected in four spectral bands: Red, Green, Blue, and Near-Infrared, providing a standard

4-band (RGBI) composition well suited for vegetation mapping and land cover classification. NAIP imagery is widely used in urban tree canopy assessments because it provides consistent, repeatable, leaf-on aerial coverage collected under a single coordinated acquisition program with uniform sensor parameters. In this study, the 2022 imagery serves as the historical reference condition against which post-Hurricane Helene canopy conditions are evaluated.

2.2.2 2025 High-Resolution Orthomosaic Imagery

The post-event dataset consists of high-resolution orthorectified imagery from 2025, including products derived from Maxar WorldView [Maxar Technologies, 2025] and Airbus Pléiades Neo 3 [Airbus Defence and Space, 2025] platforms in the 30–50 centimeter range, selected based on the best available combination of clarity, completeness, and temporal relevance. Unlike NAIP, which uses a consistent 4-band configuration across all acquisitions, these commercial sensors differ meaningfully in their spectral band configurations (see Appendix Table A2). These differences in spectral response curves contribute to radiometric disharmony when imagery from both sensors is combined into a single mosaic, with implications for classification consistency discussed further in Section 2.5.

2.3 Study Area Maps

The following figures provide the mapped study area extents for the two imagery sources used in this analysis.

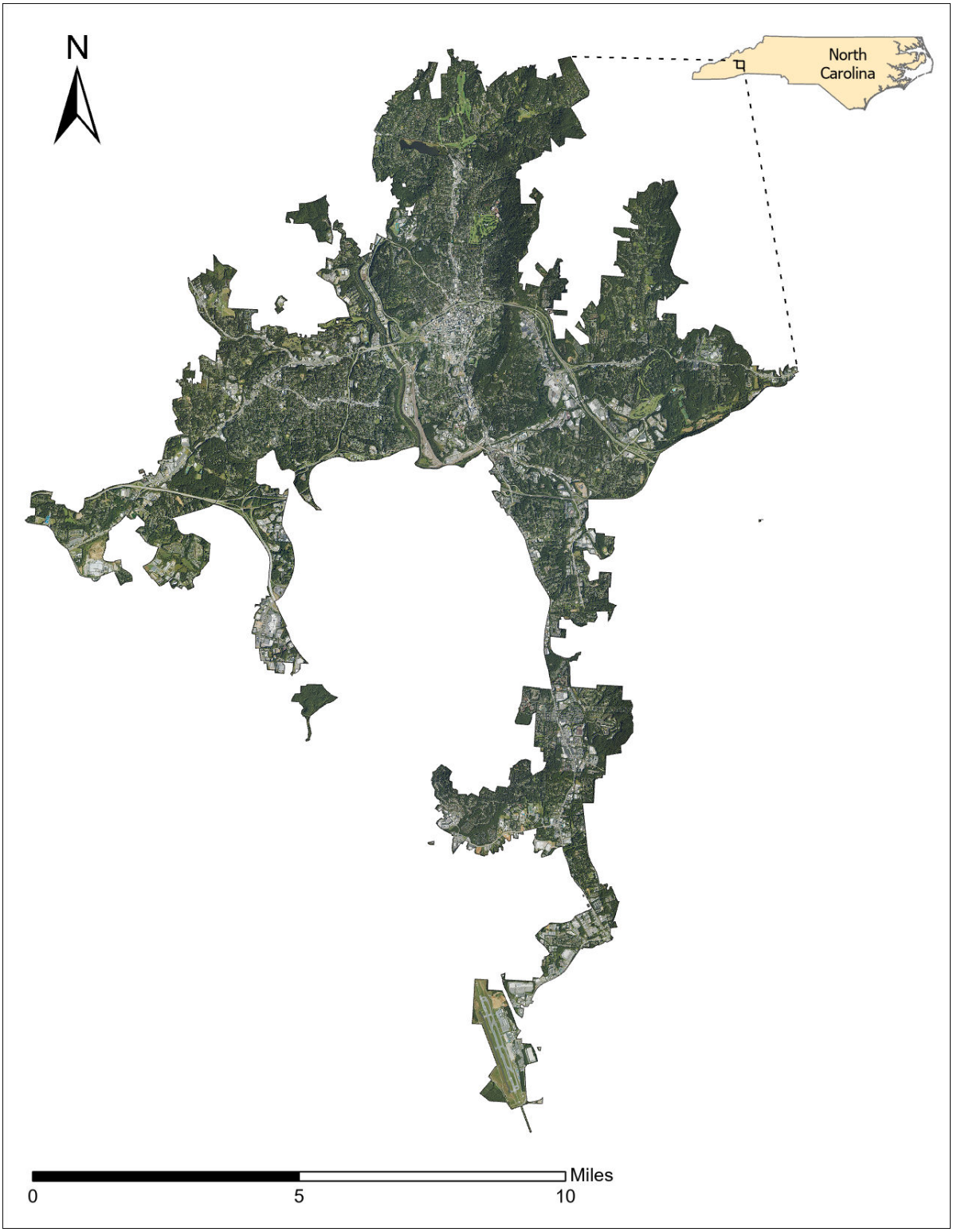


Figure 1. Study Area Map: 2022 NAIP Imagery



Figure 2. Study Area Map: 2025 High-Resolution Orthomosaic

2.4 Data Preparation and Harmonization

Both imagery datasets were preprocessed into a consistent analytical framework prior to classification. Preprocessing steps included mosaicking source imagery into continuous citywide coverage, clipping to the official Asheville study boundary, resampling both datasets to a common 1-meter spatial resolution, and reviewing imagery for cloud cover, shadow effects, and visible artifacts. The 2025 high-resolution orthomosaic was also converted from 16-bit to 8-bit radiometric depth to meet model input requirements; the 2022 NAIP imagery was already delivered as an 8-bit product.

2.5 Image Classification

Initial classification attempts were made using custom-built models trained on locally collected training samples from within the Asheville study area. These models produced poor validation scores across land cover classes and visibly degraded segmentation quality, with irregular boundaries and widespread misclassification across both vegetated and developed surfaces. Given these results, custom model development was discontinued in favor of an established pretrained solution.

Classification was performed using the Esri High Resolution Land Cover Classification – USA pretrained model, available through the ArcGIS Living Atlas of the World [Esri, 2022]. The model employs a U-Net convolutional neural network architecture, a fully convolutional encoder-decoder design commonly used for semantic segmentation of high-resolution imagery. The model was originally trained on the Chesapeake Bay 2013/2014 NAIP Land Cover dataset and is optimized for leaf-on, 4-band (RGBI) NAIP imagery at approximately 1-meter resolution. It produces six land cover output classes: water, tree canopy and shrubs, low vegetation, barren, impervious surfaces, and impervious roads.

The pretrained model was applied without fine-tuning to both the 2022 and 2025 imagery datasets. Attempts were made to fine-tune the model using locally collected training samples from within the Asheville study area; however, fine-tuned model runs produced lower validation scores across land cover classes and visibly degraded segmentation quality, with irregular boundaries and increased misclassification in both vegetated and developed areas. The unmodified pretrained model was therefore retained for all classification work, as it demonstrated stronger validation performance and more spatially coherent segmentation across both imagery datasets. Model validation performance metrics for all six output classes are provided in Appendix Table A1.

Application of the pretrained model to the 2025 high-resolution orthomosaic required an additional preprocessing step not necessary for the 2022 NAIP imagery. Initial classification runs were performed on the full citywide mosaic and produced inconsistent results across the study area. This was attributed to spectral disharmony within the 2025 dataset, which was assembled from imagery collected by multiple sensors, primarily Maxar and Airbus platforms, each with distinct radiometric characteristics and spectral response curves. Unlike the 2022 NAIP imagery, which was collected under a single coordinated acquisition program with consistent sensor parameters citywide, the 2025 orthomosaic contains radiometric discontinuities at strip boundaries where imagery from different sensors was joined. When classified as a single mosaic, these inter-sensor differences were interpreted by the model as land cover variation, producing classification artifacts along seam lines and degrading output quality across affected areas. Classification was therefore performed on individual image strips rather than the full mosaic, allowing the model to operate within spectrally consistent segments before outputs were merged into a single citywide product.

2.6 Manual Tree Canopy Clean Up

Quality review of the multi-class classification outputs revealed unacceptable error levels in several non-canopy classes. Buildings, impervious surfaces, grass and low vegetation, bare soil, and open water were therefore excluded from final deliverables. The analysis was focused exclusively on the tree canopy and shrubs class, which demonstrated the highest classification reliability across both time periods (F1-score of 0.92 on the model validation dataset).

Even within the tree canopy and shrubs class, model outputs required refinement. The *Reclassify* tool was first applied to the classified raster to isolate the tree canopy and shrubs class, remapping the canopy class value to 1 and assigning all remaining classes a NoData value. This ensured that only canopy pixels were retained prior to any editing or vectorization.

With the canopy class isolated, a pixel-level correction pass was conducted using the ArcGIS Pro *Pixel Editor*, which allowed individual misclassified pixels to be reassigned directly on the reclassified raster. This step addressed commission and omission errors in areas of deep shadow, canopy edges, and spectrally mixed surfaces, producing a cleaner raster input for the subsequent conversion step.

The corrected raster was then converted to polygon features using the *Raster to Polygon* tool, with the *Simplify* option enabled to reduce geometric complexity along polygon boundaries while preserving overall crown shape. The resulting polygon feature class contained only tree canopy and shrubs features and served as the input for all subsequent manual editing.

Final boundary refinement was conducted using the *Edit Vertices*, *Merge*, *Split*, and *Reshape* tools to correct any remaining commission and omission errors, remove residual misclassified patches, and align canopy boundaries to crown edges visible in the source imagery. Upon completion, topology validation was run to enforce no overlapping polygons before the feature class was exported for area calculation.

2.7 Data Considerations and Limitations

Several factors introduce uncertainty into this analysis that are worth noting explicitly. The two imagery datasets differ in sensor type, native spatial resolution, acquisition geometry, and radiometric characteristics, all of which can influence how vegetation and built surfaces are represented and classified. Although both datasets were resampled to a common 1-meter resolution and processed through a unified classification framework, these differences cannot be fully eliminated and may contribute to apparent canopy change that does not reflect true on-the-ground conditions.

The multi-sensor composition of the 2025 orthomosaic presented particular challenges. Radiometric discontinuities between Maxar and Airbus acquisition strips required classification to be performed on individual strips rather than the full mosaic, and some residual seam effects may persist in the final merged product. Additionally, differences in off-nadir acquisition angle between the two datasets can cause tree crowns to appear laterally displaced from their true position, introducing edge effects in the change detection output that may be misinterpreted as localized gain or loss. These effects are most pronounced along canopy edges and around tall, isolated trees.

The manual cleanup process applied to the tree canopy and shrubs class reduces but does not eliminate classification error. Some commission and omission errors likely remain, particularly in areas of deep shadow, dense mixed vegetation, or spectrally complex urban surfaces. Canopy extent figures reported here should be understood as estimates subject to these sources of uncertainty rather than exact measurements.

2.8 Role of the Data in This Assessment

The 2022 NAIP imagery and 2025 high-resolution orthomosaic together form the analytical foundation of this project. The 2022 dataset establishes the pre-storm canopy baseline against which post-Hurricane Helene conditions are measured, while the 2025 dataset captures the post-event landscape at a spatial resolution sufficient to detect fine-scale canopy loss and fragmentation. Together they enable production of canopy cover maps for each period, quantification of citywide canopy extent and change, and spatial identification of where loss is concentrated. The resulting data products are intended to support canopy recovery planning, targeted restoration prioritization, resilience strategy development, and ongoing monitoring of canopy conditions over time.

3 Urban Tree Canopy Assessment

3.1 Urban Tree Canopy Extent

Total canopy extent and proportional coverage were calculated for each classification period across the full Asheville city limits boundary (29,279.41 acres / 118.5 km^2). Proportional canopy coverage was computed as:

$$C = \frac{A_{\text{canopy}}}{A_{\text{total}}} \times 100 \tag{1}$$

where C is canopy coverage (%), A_{canopy} is the classified canopy area (acres), and A_{total} is the total municipal area (29,279.41 acres). Applying Equation (1), the 2022 NAIP classification estimated tree canopy at 49.51% (14,496.34 acres) and the 2025 Maxar/Airbus classification estimated canopy coverage at 47.00% (13,760.59 acres).

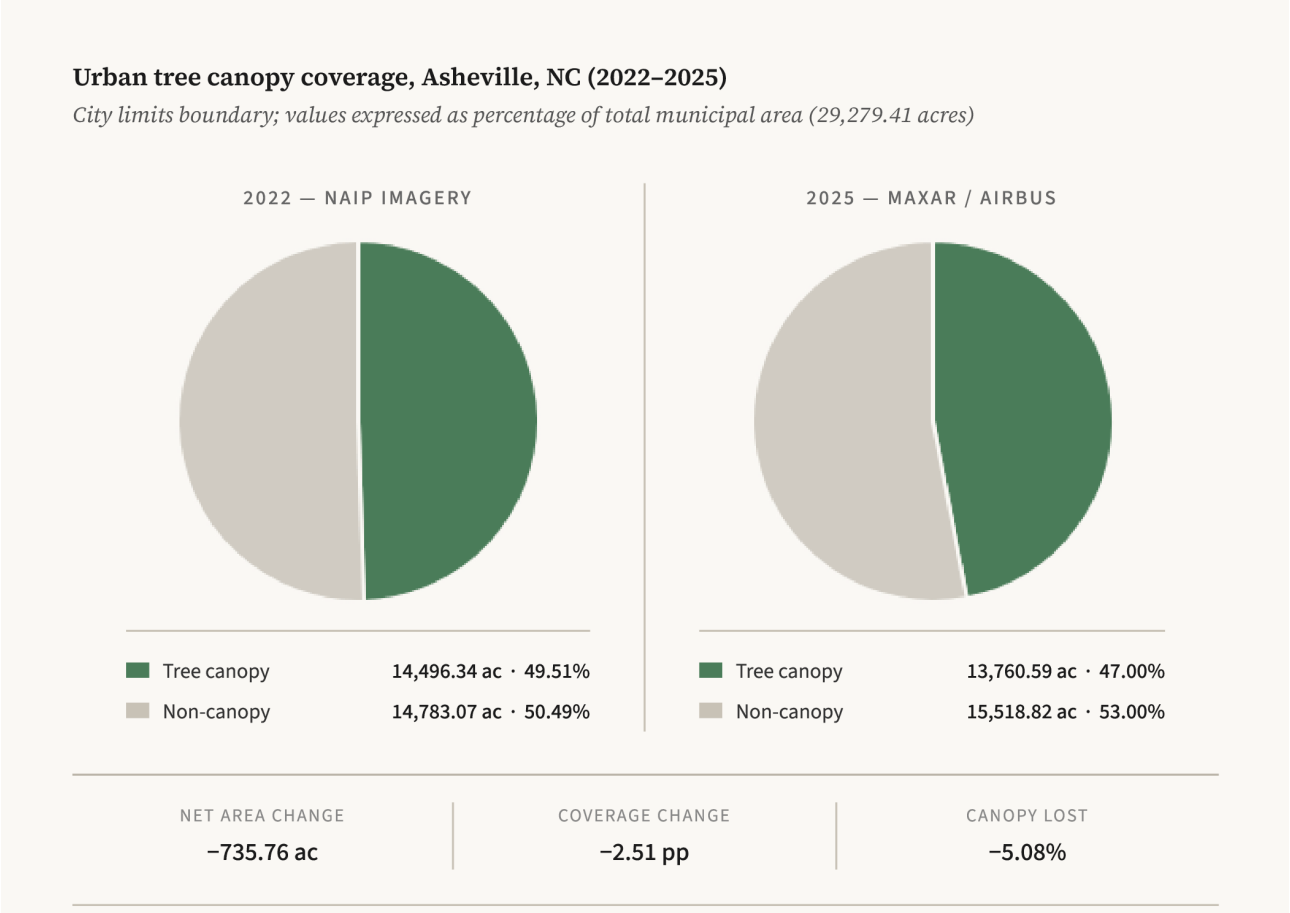


Figure 3. Urban tree canopy coverage, Asheville, NC (2022–2025)

3.2 Canopy Change Analysis

Within the Asheville city limits, canopy coverage declined from 49.51% (14,496.34 acres) in 2022 to 47.00% (13,760.59 acres) in 2025. The net change in canopy area was calculated as:

$$\Delta A = A_{\text{canopy},2025} - A_{\text{canopy},2022} = 13{,}760.59 - 14{,}496.34 = -735.76 \text{ acres} \tag{2}$$

The change in proportional coverage, expressed in percentage points (pp), was computed by direct subtraction of the two coverage values derived from Equation (1):

$$\Delta C = C_{2025} - C_{2022} = 47.00 - 49.51 = -2.51 \text{ pp} \tag{3}$$

Percentage points represent an absolute shift on the municipal coverage scale and are distinct from a relative percent change. The canopy lost statistic, expressed as a percentage of the 2022 canopy extent, was computed as:

$$L = \frac{|\Delta A|}{A_{\text{canopy},2022}} \times 100 = \frac{735.76}{14{,}496.34} \times 100 \approx 5.08\% \tag{4}$$

where L is the proportion of 2022 canopy area lost, $|\Delta A|$ is the absolute net area change from Equation (2), and $A_{\text{canopy},2022}$ is the 2022 baseline canopy extent (14,496.34 acres). Together, Equations (2)–(4) indicate a net canopy loss of 735.76 acres (2.51 pp; 5.08% of 2022 canopy extent), as illustrated in Figure 3.

It should be noted that although both datasets were resampled to a common 1-meter spatial resolution prior to classification, differences in native imagery resolution, acquisition geometry, and radiometric characteristics between the 2022 NAIP and 2025 high-resolution orthomosaic may still influence classification outputs. Observed changes therefore likely reflect a combination of true canopy loss and residual sensitivity differences introduced by the underlying source imagery.

Spatial distributions of classified tree canopy for each time period are presented in Figures 4 and 5. The 2022 NAIP-derived canopy map (Figure 4) illustrates pre-event baseline conditions, with canopy concentrated in the outer residential and forested periphery of the city and notably reduced in the urban core. The 2025 classification (Figure 5) reflects post-Hurricane Helene conditions and, while broadly similar in spatial pattern, shows measurable reductions in canopy density across multiple areas of the city.

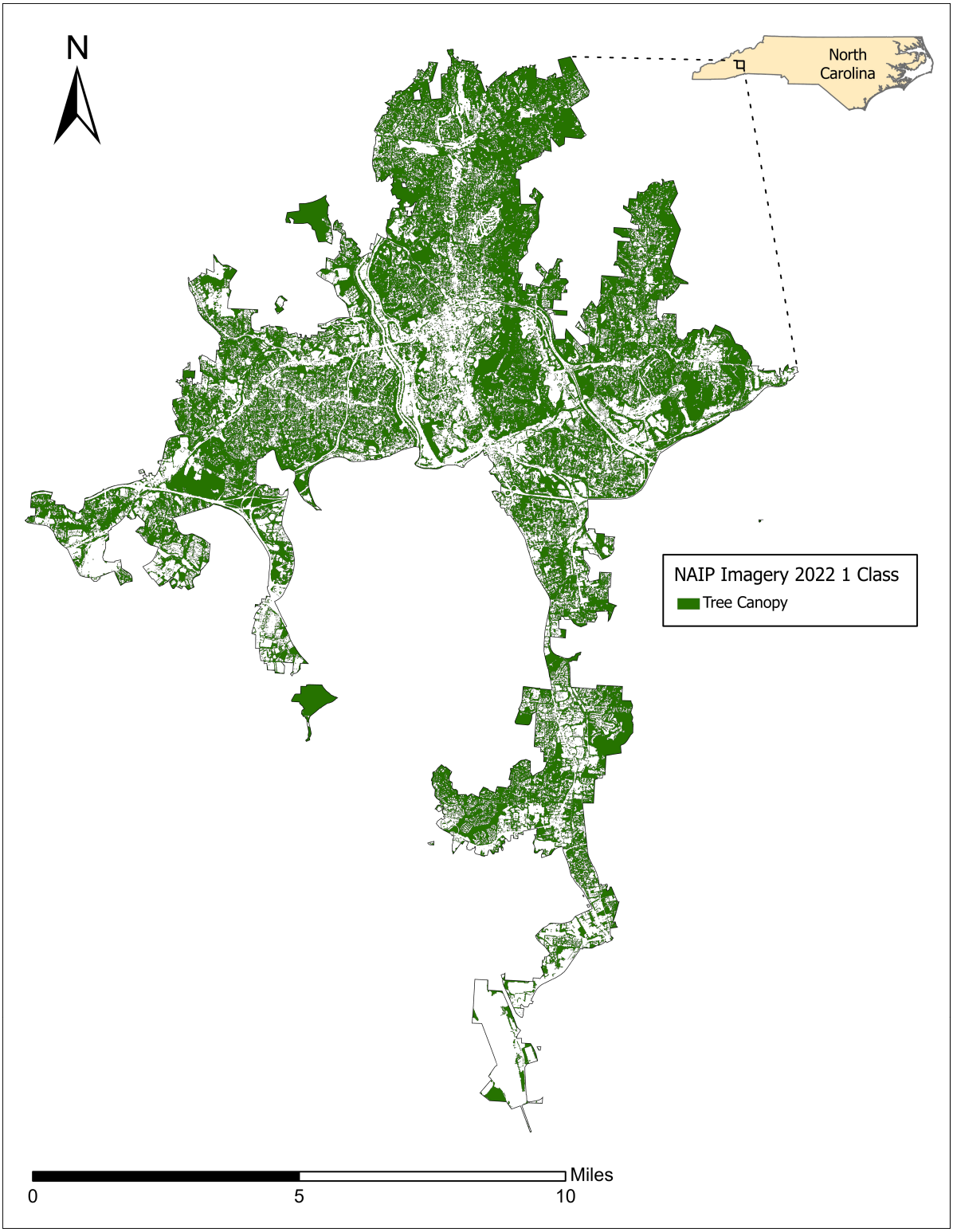


Figure 4. Classified Tree Canopy: 2022 NAIP Imagery

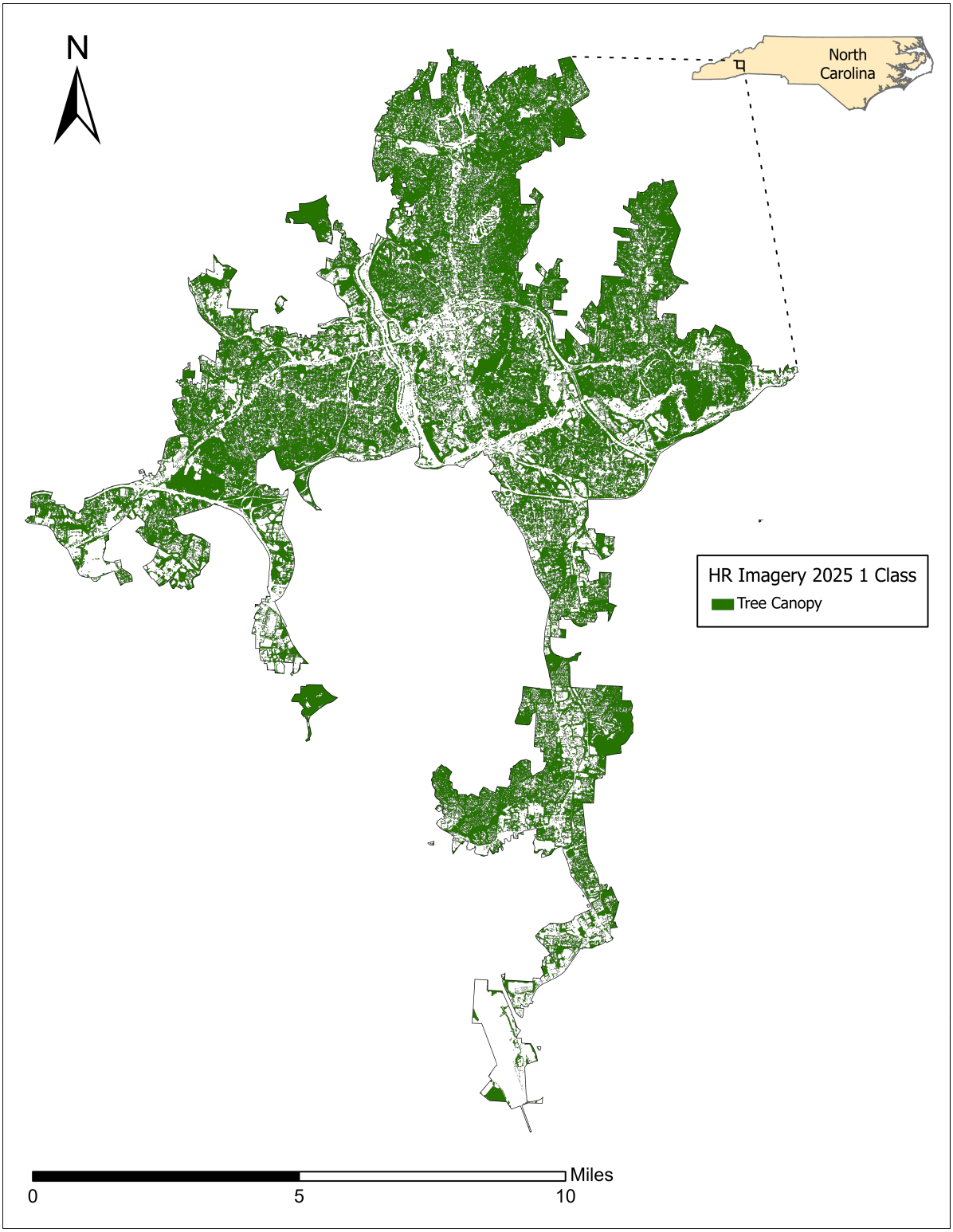


Figure 5. Classified Tree Canopy: 2025 High-Resolution Imagery

3.3 Spatial Patterns

Spatial analysis of canopy change revealed heterogeneous patterns across the study area (Figure 6). Areas of canopy loss (shown in red) are broadly distributed across the city but are notably concentrated along riparian corridors and in mid-city residential neighborhoods, consistent with documented Hurricane Helene impact zones. Canopy gain (shown in blue) is comparatively limited in spatial extent, confirming that net change across the study period is loss-dominated. It should be noted that some localized gain and loss patterns may be attributable to differences in off-nadir acquisition angle between the two imagery sources. Variations in view angle can cause tree crowns to appear displaced laterally from their true ground position, such that canopy edges shift slightly between acquisitions and are incorrectly interpreted as gain or loss during change detection. This effect is most pronounced along canopy edges and in areas of tall, isolated trees, and should be considered when interpreting fine-scale change patterns.

Four inset areas (A–D) illustrate canopy change at finer spatial scales (Figures 7a–7d). Each inset shows pre-event 2022 imagery alongside 2025 imagery with canopy loss highlighted in red. Inset A captures an area of commercial and residential land clearing where contiguous canopy was removed, consistent with active development activity rather than storm disturbance. Inset B shows a densely canopied residential neighborhood with diffuse but widespread loss across individual lots and street trees. Inset C depicts a riparian corridor and recreation area where loss follows a linear pattern along a watercourse, with canopy retained on surrounding upland slopes. Inset D shows loss concentrated along the perimeter of the regional airport and adjacent parcels. Collectively, the insets confirm that riparian and low-lying areas experienced the most severe and contiguous canopy removal, while some loss patterns reflect ongoing development pressure independent of storm impacts.

Further analysis using co-registered imagery and ancillary disturbance data would be required to definitively distinguish storm-driven canopy loss from classification variability or pre-existing land use change.

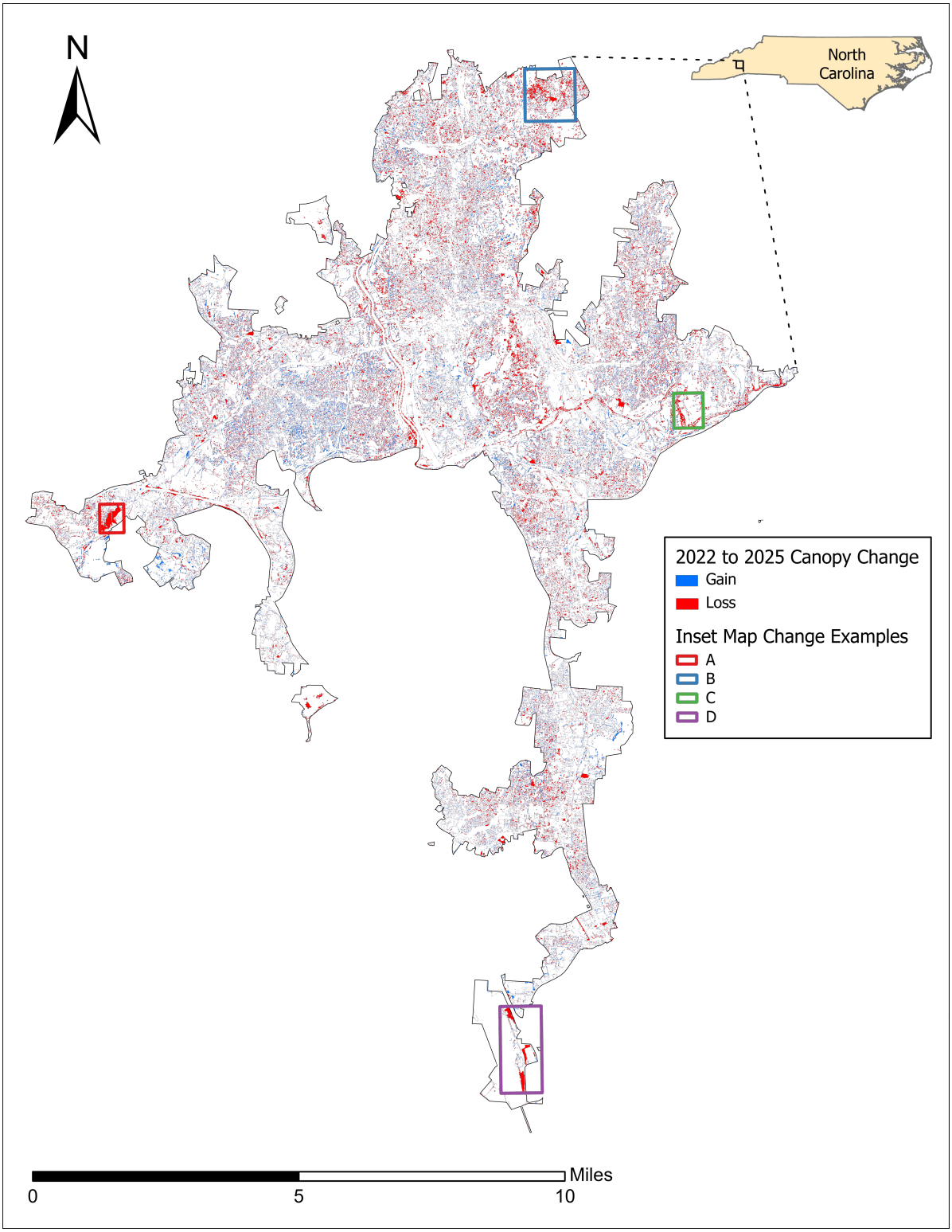


Figure 6. Canopy Change Map: 2022 to 2025. Canopy gain (blue) is shown on the 2022 NAIP imagery and canopy loss (red) is shown on the 2025 Maxar/Airbus high-resolution orthomosaic.



Figure 7a. Canopy Change Inset A: Commercial and Residential Land Clearing. Left: 2022 NAIP imagery with gain in blue. Right: 2025 Maxar/Airbus orthomosaic with loss in red.

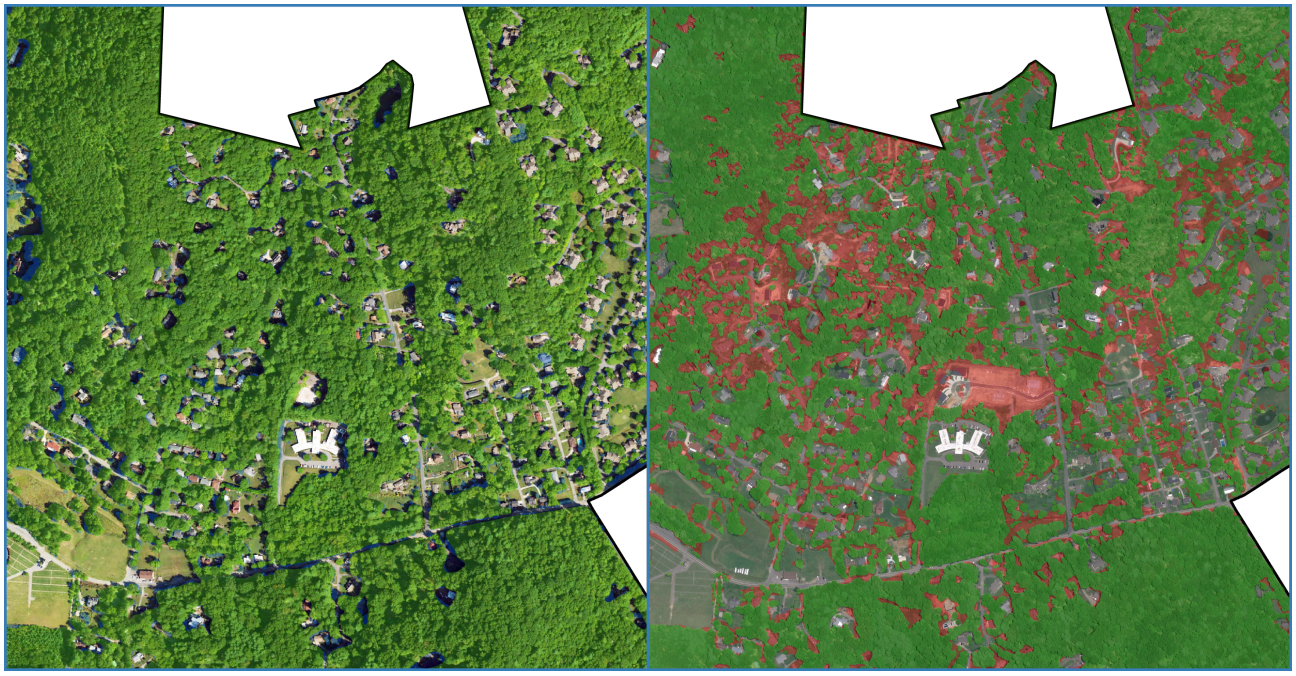


Figure 7b. Canopy Change Inset B: Residential Neighborhood Loss. Left: 2022 NAIP imagery with gain in blue. Right: 2025 Maxar/Airbus orthomosaic with loss in red.

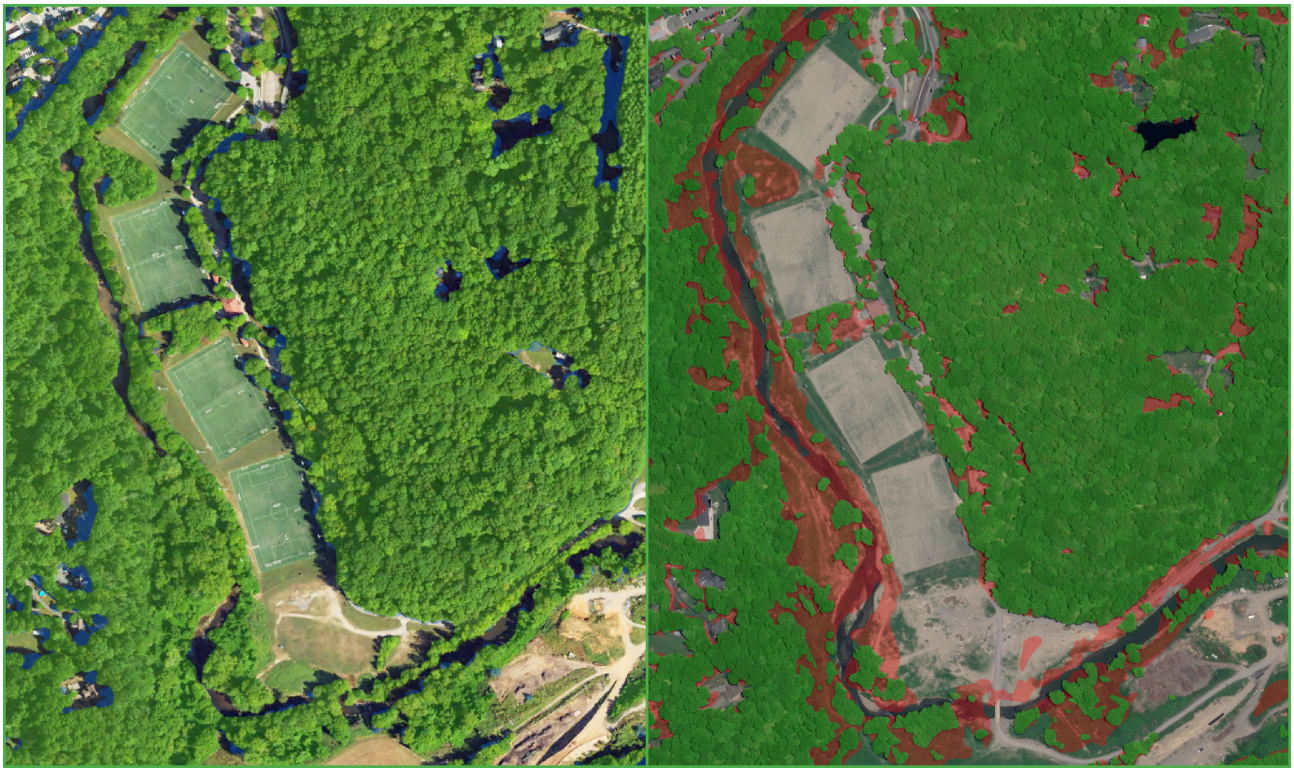


Figure 7c. Canopy Change Inset C: Riparian Corridor and Recreation Area. Left: 2022 NAIP imagery with gain in blue. Right: 2025 Maxar/Airbus orthomosaic with loss in red.

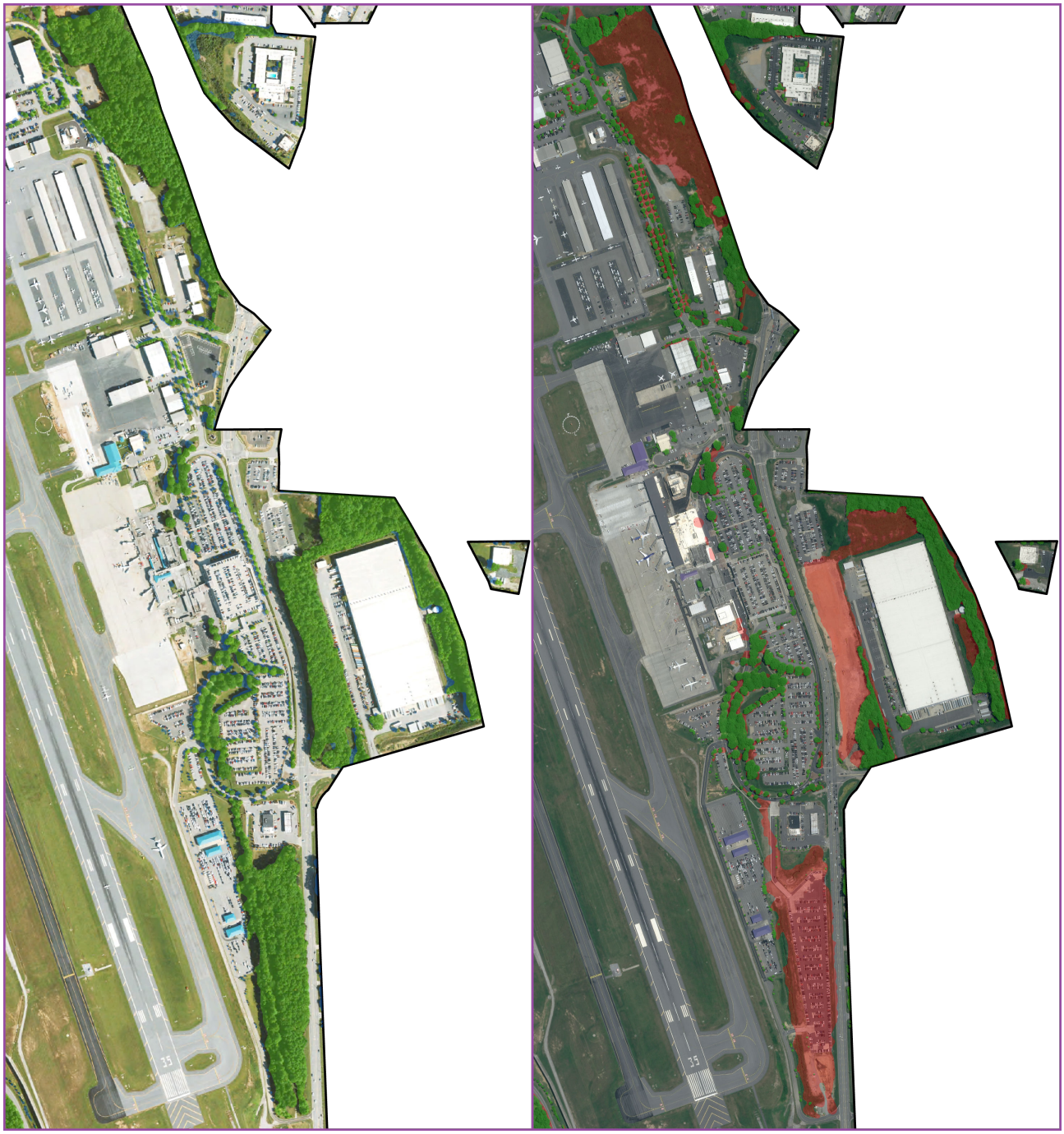


Figure 7d. Canopy Change Inset D: Airport Perimeter Area. Left: 2022 NAIP imagery with gain in blue. Right: 2025 Maxar/Airbus orthomosaic with loss in red.

4 Discussion

This assessment documents a measurable decline in urban tree canopy across Asheville following Hurricane Helene, with a net loss of 735.76 acres (2.51 pp; 5.08% of 2022 canopy extent, Equation (4)) representing a meaningful reduction in the city's pre-storm canopy cover. While some portion of the observed change may reflect differences in imagery characteristics and classification sensitivity between the two datasets, the spatial distribution of loss is concentrated in riparian corridors, residential neighborhoods, and low-lying areas consistent with known flood inundation zones, which points to storm-driven disturbance as a contributing factor.

However, a careful review of the spatial loss patterns suggests that a substantial portion of the detected canopy loss may be attributable to urban development activity rather than storm damage. Loss patches in several areas align with land clearing, new construction, and impervious surface expansion rather than the irregular, disturbance-driven patterns typically associated with wind or flood damage. Inset A (Figure 7a) provides a clear example of this, where canopy loss is concentrated in an area consistent with commercial and residential development activity rather than storm impact. Some loss in riparian and low-lying areas may be storm-related, but without additional ancillary data it is difficult to attribute loss with confidence to any single cause. This is an important distinction for recovery planning, as development-related loss reflects ongoing land use pressure that will continue to erode canopy cover independent of storm events.

Canopy gain identified over the study period is limited and likely reflects opportunistic vegetation growth in previously open areas rather than any active restoration. It is also worth noting that a portion of the detected gain may not represent true on-the-ground change. Differences in off-nadir acquisition angle between the two imagery sources can cause tree crowns to appear shifted from their actual position, with canopy edges registering as gain in one period where they appeared as loss in another. As a result, some of the gain signal, particularly along canopy edges and around tall isolated trees, should be interpreted with caution. The data nonetheless suggest that natural recovery alone will not be sufficient to offset losses in the near term, and that targeted replanting will be needed to restore pre-storm canopy levels.

The classification challenges encountered during this project offer useful guidance for future assessments. Two separate modeling approaches were attempted: first, custom models were built from scratch using locally collected training samples, and second, the Esri pretrained model was fine-tuned using the same local samples. Both efforts were unsuccessful, yielding poor validation scores and degraded segmentation quality. The multi-sensor composition of the 2025 orthomosaic introduced an additional complication, as radiometric differences between Maxar and Airbus imagery caused classification artifacts when the model was applied to the full mosaic. Processing the imagery by individual acquisition strip rather than as a single citywide product was necessary to obtain consistent results. These challenges are consistent with the known difficulty of applying land cover models to high-resolution commercial imagery assembled from heterogeneous sensor sources, where spectral variability between acquisitions can be as significant as variability between land cover classes. For future work involving similar datasets, restricting model scope to tree canopy classification alone is recommended. A binary canopy versus non-canopy framing reduces class overlap, simplifies the decision boundary, and is more likely to yield reliable, transferable results than a full multi-class approach given the spectral and structural complexity inherent to high-resolution urban imagery.

The spatial data developed through this assessment can help the city prioritize where recovery

efforts are most needed. Distinguishing between storm-driven and development-driven loss will be an important next step, and could be supported by overlaying the canopy change data with building permits, land use records, and parcel activity from the study period. Periodic re-assessment using updated imagery will be important for tracking canopy recovery and evaluating the effectiveness of restoration efforts over time.

5 Appendix

Table A1. Model Validation Performance: Esri High Resolution Land Cover Classification – USA

The table below summarizes the precision, recall, and F1-score of the Esri pretrained U-Net model on the validation dataset, evaluated across all six land cover output classes. Classification was applied to both the 2022 NAIP and 2025 high-resolution orthomosaic datasets. Only the tree canopy and shrubs class was retained for final canopy analysis (see Section 2.6).

Table A1. Esri High Resolution Land Cover Classification Model Validation Metrics

Class	Precision	Recall	F1-Score
Water	0.95	0.94	0.95
Tree Canopy and Shrubs	0.91	0.92	0.92
Low Vegetation	0.85	0.85	0.85
Barren	0.79	0.69	0.74
Impervious Surfaces	0.84	0.84	0.84
Impervious Roads	0.82	0.83	0.82

Source: Esri, ArcGIS Living Atlas of the World. High Resolution Land Cover Classification – USA pretrained model validation results.

Table A2. Imagery Source Spectral Band Configurations

The table below summarizes the spectral band configurations for each imagery source used in this assessment. Dashes indicate bands not present in that sensor's configuration. Spectral band differences between Maxar and Airbus sensors contributed to the classification challenges described in Section 2.5.

Table A2. Spectral Band Configurations by Imagery Source

Band	NAIP (2022)	Maxar WorldView	Airbus Pléiades Neo 3
Coastal/Deep Blue	—	400–450 nm	400–450 nm
Blue	450–510 nm	450–510 nm	450–520 nm
Green	510–580 nm	510–580 nm	530–590 nm
Yellow	—	585–625 nm	—
Red	620–690 nm	630–690 nm	620–690 nm
Red Edge	—	705–745 nm	700–750 nm
Near-Infrared	770–880 nm	770–895 nm	770–880 nm
Near-IR 2	—	860–1040 nm	—
Panchromatic	—	450–800 nm	450–800 nm

Sources: USDA Farm Service Agency (NAIP); Maxar Technologies (WorldView); Airbus Defence and Space (Pléiades Neo 3).

References

Airbus Defence and Space. Pléiades neo 3 satellite imagery. Commercial high-resolution satellite imagery, 2025. URL https://www.intelligence-airbusds.com/imagery/constellation/pleiades-neo/.

Esri. High resolution land cover classification – USA. Pretrained deep learning model, ArcGIS Living Atlas of the World, 2022. URL https://doc.arcgis.com/en/pretrained-models/latest/imagery/introduction-to-high-resolution-land-cover-classification-usa.htm.

Maxar Technologies. Worldview satellite imagery. Commercial high-resolution satellite imagery, 2025. URL https://www.maxar.com/products/satellite-imagery.

USDA Farm Service Agency. National agriculture imagery program (NAIP). Aerial imagery program, U.S. Department of Agriculture, 2022. URL https://www.fsa.usda.gov/programs-and-services/aerial-photography/imagery-programs/naip-imagery/.